Cyclotron Production of 225Ac from an electroplated 226Ra Target

Kotaro Nagatsu (nagatsu.kotaro@qst.go.jp)
National Institutes for Quantum and Radiological Science and Technology: Kokuritsu Kenkyu Kaihatsu Hojin Ryoshi Kagaku Gijutsu Kenkyu Kaihatsu Kiko

Hisashi Suzuki
National Institutes for Quantum and Radiological Science and Technology: Kokuritsu Kenkyu Kaihatsu Hojin Ryoshi Kagaku Gijutsu Kenkyu Kaihatsu Kiko

Masami Fukada
National Institutes for Quantum and Radiological Science and Technology: Kokuritsu Kenkyu Kaihatsu Hojin Ryoshi Kagaku Gijutsu Kenkyu Kaihatsu Kiko

Taku Ito
Nihon Medi-Physics Co Ltd: Nihon Medi-Physics Kabushiki Kaisha

Jun Ichinose
Nihon Medi-Physics Co Ltd: Nihon Medi-Physics Kabushiki Kaisha

Yoshio Honda
Nihon Medi-Physics Co Ltd: Nihon Medi-Physics Kabushiki Kaisha

Katsuyuki Minegishi
National Institutes for Quantum and Radiological Science and Technology: Kokuritsu Kenkyu Kaihatsu Hojin Ryoshi Kagaku Gijutsu Kenkyu Kaihatsu Kiko

Tatsuya Higashi
National Institutes for Quantum and Radiological Science and Technology: Kokuritsu Kenkyu Kaihatsu Hojin Ryoshi Kagaku Gijutsu Kenkyu Kaihatsu Kiko

Ming-Rong Zhang
National Institutes for Quantum and Radiological Science and Technology: Kokuritsu Kenkyu Kaihatsu Hojin Ryoshi Kagaku Gijutsu Kenkyu Kaihatsu Kiko

---

Research Article

Keywords: Actinium-225, Radium-226, Alpha emitter, Targeted alpha therapy

Posted Date: March 4th, 2021

DOI: https://doi.org/10.21203/rs.3.rs-276600/v1

Version of Record: A version of this preprint was published at European Journal of Nuclear Medicine and Molecular Imaging on July 1st, 2021. See the published version at https://doi.org/10.1007/s00259-021-05460-7.

Abstract

Purpose

We demonstrate a cyclotron production of high-quality ^{225}Ac using an electroplated ^{226}Ra target.

Methods

All ^{226}Ra used in this work was extracted from legacy Ra sources using a chelating resin. The subsequent ion-exchange purification gave pure ^{226}Ra with a certain amount of carrier Ba. The radium target was prepared by electroplating. We successfully deposited about 1 mg (mCi) of ^{226}Ra on a target box. Activation was performed by 16.5 MeV protons (on the target) at 20 μA for 5 h as the maximum. Purification of ^{225}Ac as well as ^{226}Ra recovery was performed using two functional resins with various concentrations of nitric acid. Cooling of the intermediate ^{225}Ac for 2–3 weeks decayed the major byproduct of ^{226}Ac and increased the radionuclidic purity of ^{225}Ac. Then the same separation protocol was repeated to provide high-quality ^{225}Ac.

Results

We obtained ^{225}Ac at a yield of about 2.4 MBq (65 μCi) at EOB, and the subsequent primal purification gave 1.7 MBq (48 μCi) of ^{225}Ac with ^{226}Ac/^{225}Ac ratio of < 4% at 4 d from EOB. Additional cooling time coupled with the repeated separation procedure (secondary purification) effectively increased the ^{225}Ac (4n + 1 series) radionuclidic purity up to 99+%, which showed a similar identification to a commercially available ^{225}Ac originating from a ^{229}Th/^{225}Ac generator.

Conclusion

The ^{226}Ra(p,2n)^{225}Ac reaction and the appropriate purification procedure has the potential to be a major alternative pathway for ^{225}Ac production and can be performed in any facility with a compact cyclotron to address the increasing demand for ^{225}Ac.

Introduction

Targeted alpha therapy (TAT), a therapeutic regimen by radiopharmaceuticals labeled with alpha emitters, has received great interest due to the clinical impact such as $^{223}RaCl_2$ and ^{225}Ac-PSMA-617 [1, 2]. Compared to conventional targeted radionuclide therapy by beta emitters, a high linear energy transfer (LET) in a short range (40–100 μm / 5–9 MeV, [3]) is a favorable property of alpha particles, which may

provide a remarkable cytotoxic effect in a limited area of the target. Hence, unwanted radiation doses to other healthy tissues and organs may be limited.

The accessibility of various radioisotopes for diagnostic nuclear medicine is well established. Short-lived ones are produced by an in-house accelerator, while those with longer half-lives are commercially distributed at nearly on demand. On the other hand, a shortage of ^{225}Ac is expected [4], because accessibility of ^{225}Ac is limited and large-scale commercial production is in the development phase, but interest has drastically risen. Many reports on the ^{225}Ac production describe that the most realistic current practice in the supply of ^{225}Ac is relying on the natural decay product by ^{229}Th/^{225}Ac generator system [5, 6] stocked in few institutes, i.e., Joint Research Centre (JRC, Karlsruhe, Germany), Oak Ridge National Laboratory (ORNL, TN, USA), and Institute of Physics and Power Engineering (IPPE, Kaluga Oblast, Russia); and their annual capacity of total ^{225}Ac supply is estimated to be approximately 63 GBq (1.7 Ci) [7]. Consequently, artificial production pathways of ^{225}Ac are highly desired.

Many studies on the artificial ^{225}Ac production have demonstrated or planned with high potential to address the increasing demand. Practical options include (1) high-energy protons on ^{232}Th (spallation channel, [8]), (2) moderate energy protons on ^{226}Ra (nuclear transmutation channel, [9]), and (3) high-intensity gammas on ^{226}Ra (photonuclear/ Bremsstrahlung channel, [10–12]). Among them, option (1) holds promise because ^{232}Th is not a fissile material with regard to nuclear regulations, but the reaction requires a projectile with extraordinarily high energy and intensity (e.g., 100 MeV or higher proton) to perform this spallation channel efficiently. Consequently, very few facilities can practically produce ^{225}Ac via this route. On the other hand, options (2) and (3) use ^{226}Ra as their target material. While nasty issues (i.e., radon (^{222}Rn) emanation and high-energy gamma emission from the descendants) make handling this material difficult, option (2) can be advantageous when planning ^{225}Ac production in general facilities. For instance, as reported in [9], the reaction of ^{226}Ra(p,2n)^{225}Ac can be performed efficiently with relatively low amount of ^{226}Ra in a low-energy window, which can be provided by medical compact cyclotrons, Ep ≤ 20 MeV. In this study, we evaluate the production feasibility of ^{225}Ac from a ^{226}Ra target that includes (1) ^{226}Ra recovery from legacy needles, (2) radium target preparation, (3) activation, (4) separation chemistry, and (5) recycling of ^{226}Ra. This report should be beneficial when considering the production capability as well as quality control for further large-scale ^{225}Ac production.

Materials And Methods

Materials

Hydrochloric acid (ultra-pure, 10 M) was purchased from Kanto Chemical Corporation (Tokyo, Japan). Ammonium acetate solution (10 M) was obtained from Nacalai Tesque (Kyoto, Japan). Ammonium solution (25%), nitric acid (70%), pure water, Dowex Monosphere 550A anion exchange resin (OH form, 590 ± 50 μm), and Dowex AG1-X8 anion exchange resin (Cl form, 100–200 mesh) were obtained from

FUJIFILM Wako Chemicals (Tokyo, Japan). These reagents were used as received or diluted with the appropriate volume of pure water, as needed. Chelex-100 (Na form, 100–200 mesh) was purchased from Bio-Rad Laboratories (Tokyo, Japan). It was preconditioned as the ammonium form before use. Actinium-225 nitrate (37 MBq, 99.99% radionuclidic purity) was purchased from Oak Ridge National Laboratory and used as an authentic ^{225}Ac source.

Methods

General

All the following procedures were performed in a ventilated glove box. Inside pressure of the glove box was set at negative 50 Pa, and no specific system for ^{222}Rn handling was installed. A bag-in/out protocol with polyethylene bag (thickness 100 μm) was employed when transferring samples across the glove box to avoid releasing ^{222}Rn and other possible radioactive materials into laboratory [Online Resource 1–3]. The maximum daily permission for handling ^{226}Ra in our laboratory is 148 MBq (4 mCi).

Ra recovery from legacy needles

Radium needles (∅1.6 × 25 mm; 1–2 mCi-^{226}Ra/needle) were sectioned into 5–6 pieces by an ordinal tube cutter (nipper type, for 1/16” stainless tubes). The pieces, which were collected in a 50-mL glass bottle with a polypropylene screw cap (Duran Wheaton Kimble, Germany), were mixed with 3 mL of a Chelex-100 resin slurry and 7 mL of pure water. The tightly capped bottle was sonicated daily for a period of one week to one month. Additional processes were not conducted.

Afterward, the Chelex-100 resin was filtered from those mixed materials by an empty cartridge (Bond Elut, 5 mL, Agilent Technologies, CA, USA), where the extracted ^{226}Ra had been adsorbed on the resin. Then 1 M HCl (5 mL) and subsequent pure water (10 mL) for rinsing were loaded into the cartridge to elute ^{226}Ra from Chelex-100. The eluant was loaded into an anion exchange resin (16 mL, Monosphere) to remove chlorides. Then the resin was washed with 10 mL pure water. The recovered solution was evaporated at 130°C under a vacuum, yielding dried ^{226}Ra in the hydroxide form.

If the activity of the mixture of needle pieces and Chelex-100 residue was above a certain threshold, the mixture was returned to the bottle. To ensure the Chelex-100 function for adsorbing ^{226}Ra effectively, a portion of conc. ammonium solution was added to adjust the pH of the slurry ≥ 10, and the same procedure was carried out repeatedly.

Target box design and target preparation

The ^{226}Ra target is prepared by electrodeposition. Figure 1 shows the target box assembly. A Ti cylindrical cavity (#3 in Fig. 1) with a volume of about 3.5 mL was used for the reservoir for electroplating and the dissolving vessel for the Ra target after activation. A Pt rod (∅3 mm, anode for electroplating) was held by a polyimide-made screw with O-rings (#7). The bottom of the Ag cavity (#5) was assembled with both #3 and a polyimide electric insulator (#4). It should be noted that the Ra-depositing surface

with a conical shape (#5) was fabricated with Au by hot isostatic pressing on the Ag body to ensure chemical resistance.

Purified dried ^{226}Ra, which ranged from 400 to 1050 μCi (or μg on the weight scale), was dissolved in 1 mL of 0.1 M HCl and 2 mL of 0.5 M ammonium acetate to prepare the electrolyte. The electrolyte was placed in the target box, and a constant current of 100 mA DC was applied in the pulse mode (5 Hz, on in 0.1 s and off in 0.1 s) for 3 h with a 15-mm gap between the cathode and the anode. After the electrodeposition process, the electrolyte was removed from the cavity by pipette work, and introduced in and removed from 2 mL of pure water twice to wash out the residual electrolyte. These solutions, which may contain undeposited free ^{226}Ra, were collected. Then the deposition efficiency was evaluated by measuring the ^{226}Ra activity. The cavity stood undisturbed overnight (> 15 h) to dry the Ra surface naturally in a ventilated glove box. Eventually, the Pt anode was withdrawn from the cavity and sealed with a thin Nb foil (50 μm). The cavity at the beam entrance was sealed with a 50-μm-thick Nb foil (#2 in Fig. 1) with #1.

Activation

Activations were carried out by 34 MeV H_2^+ (ionized molecular hydrogen) provided by NIRS-AVF-930 cyclotron at a nominal intensity of 10 μA for 3–5 h. This condition increased the intensity of lower energy particles accelerated by a relatively larger cyclotron to give 17 MeV protons at nearly 20 μA by splitting of the kinetic H_2^+ ion at the vacuum isolation window. The estimated proton energy on the target material was 15.6 MeV by passing through the vacuum foil (Al, 100 μm), the He cooling layer (30 mm), and the target foil (Nb, 50 μm).

To enrich the expected ^{225}Ac yield as much as possible, the proton energy was set slightly higher than the energy for the estimated highest cross-section of the ^{226}Ra(p,2n)^{225}Ac [9]. In the case where Ra increases, this activation condition is applicable directly, and a minimal difference is expected in the yield and radionuclidic purity of ^{225}Ac.

Separation of ^{225}Ac from the target matrix

Figure 2 shows our newly developed separation procedure, which was implemented 3–4 days after the end of bombardment (EOB). The eluent concentration was determined to be a thinner condition that does not affect the separation performance, considering ease of handling, reduction of corrosion risk to the equipment (automation to be performed in our future study), and to carry out the purification process repeated twice by the same procedure. The activated target was dissolved in 3 mL of 0.7 M HNO_3, and the solution was loaded slowly into a DGA cartridge (*N,N,N′,N′*-tetra-*n*-octyldiglycolamide, 1 mL, Eichrom Technologies, IL, USA). To increase the recovery of leftover of Ac/Ra, another 3 mL of 0.7 M HNO_3 was introduced into the target cavity twice and the respective rinsing fractions were also loaded into the same DGA cartridge.

The DGA cartridge was washed with 20 mL of 0.7 M HNO_3 to remove residual ^{226}Ra. Then 5 mM HNO_3 (10 mL) was loaded into the DGA to elute ^{225}Ac, which is the fraction collected in an intermediate reservoir. Subsequently, the crude ^{225}Ac fraction was loaded into a LN cartridge (di(2-ethylhexyl)orthophosphoric acid, 2 mL, Eichrom Technologies), the cartridge was washed with 10 mL of 50 mM HNO_3 to eliminate trace amounts of ^{226}Ra, and then well purged. All the above waste fractions were collected as the Ra recovery fraction, which was recycled for the next use. Eventually, ^{225}Ac was stripped by loading 0.7 M HNO_3 (10 mL) and collected into another intermediate reservoir.

The actinium-225 solution in this separation step contained by-produced ^{226}Ac (β 83%, EC 17%, α 6×10^{-3}%; $T_{1/2}$ = 29.4 h), which was unavoidably generated via the $^{226}Ra(p,n)$-channel in our activation condition. To increase the radionuclidic purity of ^{225}Ac, the intermediate product was allowed to cool for 2–3 weeks, which is equivalent to 10 half-lives or more for ^{226}Ac. After the cooling, the above separation protocol was repeated as the secondary purification.

Although the twice purified ^{225}Ac was free from or had negligible ^{226}Ac contamination in 0.7 M HNO_3 (10 mL), it was too acidic for further use. Thus, an anion exchange resin (AG1-X8, 100–200 mesh, Cl form) was employed to exchange the counter anion of ^{225}Ac with chloride and remove HCl from the product by evaporation of the above sample (130°C under vacuum). The final product, which was in a chemical form of $^{225}AcCl_3$, was reconstituted in a buffer and volume for further use.

Recycle mode for Ra

All fractions possibly containing ^{226}Ra were collected into a single vessel. The solution was adjusted to a pH ≥ 10 by adding conc. ammonium solution and then loaded into a column filled with the Chelex-100 resin (0.5 mL, NH_4 form) to concentrate ^{226}Ra. After washing the column with 10 mL of pure water, ^{226}Ra was stripped by passing 1 M HCl (5 mL), and the eluant was led to an anion exchange resin column directly (16 mL, Monosphere, OH form). The Ra fraction was desalted by the anion exchanger, and an additional 10 mL of pure water was loaded to wash out the residual ^{226}Ra. The collected ^{226}Ra with a volume of about 15 mL was subsequently evaporated at 130°C under a vacuum to yield purified ^{226}Ra in the hydroxide form, which was ready for the next use as the electrolyte.

Results

Ra liberation from legacy needles

In most cases, the ^{226}Ra prepared in the radium needle had a form of $RaSO_4$. Despite being an ionic compound, which is typically very soluble, Group II sulfates, including $RaSO_4$, are practically insoluble in water. Actually, our samples showed a nearly zero recovery of free $^{226}Ra^{2+}$ when the Ra matrix was suspended in water or 1 M HCl, providing additional evidence that Ra is in the sulfate. However, when Chelex-100 was allowed to sit long term, a remarkable recovery occurred as trace amounts of Ra^{2+} were

gradually liberated from the sulfate as the chelation sites tightly held Ra^{2+}. Sonication seemed to effectively pulverize or rake out a solid Ra matrix that stayed in a small cavity. Both of these situations increased the contact chance of the Ra matrix to the Chelex-100 resin. The recovery rate of ^{226}Ra was 30–50% for a week, but quantitative after a month.

Electrodeposition and Activation of ^{226}Ra

The deposition rate of ^{226}Ra was satisfactory. It ranged from 94 to 97%, as evaluated by the balance of the ^{226}Ra activity between the initial and the post-deposition electrolyte (Table 1). The deposited ^{226}Ra layer, which contained some amount of carrier Ba, was practically insoluble upon washing after the deposition process. The washing fractions of pure water showed a very small activity of ^{226}Ra (1–2% of the initial value).

Since we handled ^{226}Ra in a small amount of 400–1000 μg (μCi), the conical design of the cathode effectively enriched the Ra layer at the center of the target (Fig. 3(a)). The gap between the top of the cathode cone and the Pt anode was the shortest distance for efficient growth of the Ra layer at the center of the cone. Because the beam was generally focused at the center of the target, thick areas of the projectile and the target were expected to match and contribute to efficient activation.

A magnified image of the cathode surface showed that many precipitants were grown, spreading in random spots (Fig. 3(b)). The uneven Ra-deposition was mainly attributed to the small amount of ^{226}Ra. An uneven target would decrease the ^{225}Ac yield compared to an ideal surface with the same amount (activity) of ^{226}Ra because incoming projectiles trajected at a thin area of ^{226}Ra do not contribute to activating the target. Hence, we evaluated the deposition covering rate by a digital imaging processor (ImageJ, NIH, MD, USA [13]) to estimate a practical cross-section and our activation efficiency. Briefly, a magnified image of the target surface was acquired after electrodeposition, and the raw image was converted to an eight-bit monochrome, where white is the Ra deposition and black is the background (Fig. 3(c)). Then the coverage rate was calculated. Several parameters were set automatically to the determined default values. For run #2, which had a sample with a target of ~ 1000 μCi-^{226}Ra, the estimated coverage ratio was 64%. Hence, an ^{225}Ac yield of approximately 1/3 that of the theoretical value would be acceptable in the confirmed range up to 1-mg Ra. Increasing ^{226}Ra should alter the coverage profile, which is a subject in our future scale-up production study.

Table 1 shows the production results (three runs). Our ^{226}Ra target prepared on the cathode surface can be regarded as a thin target of 1.0–1.5 mg/cm^2. The estimated cross-section (σ) for the $^{226}Ra(p,2n)^{225}Ac$ was 353 mb at 15.6 MeV [Online Resource 4]. Previous studies showed much higher values of about 710 mb at 16.8 MeV [9], > 600 mb at 16.0 MeV calculated by ALICE code [9], and 522 mb at 16.0 MeV by TENDL-2019 [15]. However, only about 2/3 of our target's surface was unevenly covered with ^{226}Ra. Hence, the above σ can be multiplied by 1.56 (= 1/0.64), for example. Consequently, corrected values of 552 mb and 14 mb were obtained as the estimated cross-sections for the $^{226}Ra(p,2n)^{225}Ac$ and

^{226}Ra(p,n)^{226}Ac in our practical condition, respectively (cf. 34 mb for the (p,n)-channel at 16 MeV, [15]). Because the Ac separation efficiency, beam profile, or Ba/Ra ratio may introduce errors in the evaluation, quantitative corrections of such factors could not be applied in this study. Although these uncertainties were not included in the above estimation, the corrected cross-sections agreed well with the calculated values by both ALICE and TENDL codes as well as the practical value of the previous study.

Separation

The primal separation of the ^{225}Ac sample contained ^{226}Ac and other radionuclidic impurities [Fig. 4(a)]. Similar to ^{226}Ra, ^{226}Ac is a 4n + 2 series radionuclide, which generated many descendants during the cooling period. Hence, repeated separation as a secondary purification removed the 4n + 2 impurities to yield high-quality ^{225}Ac. Regarding our activation condition, although ^{224}Ac (EC 91%, α 9%, $T_{1/2}$ = 2.8 h) should be co-produced via the ^{226}Ra(p,3n)-channel (E_{TH} = 13.6 MeV), the half-life of ^{224}Ac was too short to be detected at the end of separation at 4 d from EOB. However, a couple of ^{224}Ac descendants with favorable gamma emissions in the 4n series, ^{212}Bi ($T_{1/2}$ = 61 min, 727 keV, 6.7%) and ^{208}Tl ($T_{1/2}$ = 3.1 min, 2615 keV, 99%), were the major distributions in both the washing fraction and leftover in separation materials. Moreover, trace amounts were detected in the purified ^{225}Ac sample, providing evidence for the generation of ^{224}Ac. The presence of ^{212}Bi and ^{208}Tl in the ^{225}Ac fraction was acceptable because Bi showed partial similarity to Ac in our separation conditions. On the other hand, ^{212}Pb ($T_{1/2}$ = 10.6 h, 239 keV, 44%), a parent nuclide for ^{212}Bi, was not detected in the purified ^{225}Ac samples. All the 4n series-nuclides with the potential to be the parent for ^{212}Pb (^{224}Ac–^{216}Po, except ^{224}Ra) have shorter half-lives than ^{212}Pb, and ^{224}Ra was removed along with ^{226}Ra. Hence, only the 4n + 2 series can be considered as the byproducts to be focused on in the separation process.

Other notable by-products were ^{135}La (EC, $T_{1/2}$ = 19.5 h) and ^{140}La (β, $T_{1/2}$ = 1.68 d). The former presumably originated from a possible carrier of natural Ba in the legacy Ra needle via the ^{135}Ba(p,n)-channel. However, the half-life of ^{135}La is much shorter than that of ^{225}Ac. Thus, an appropriate cooling time would gradually decrease the impact of ^{135}La on the ^{225}Ac even though the legacy Ra was not chemically purified. On the other hand, since the heaviest stable isotope of Ba is ^{138}Ba, the atomic mass of ^{140}La seemed to be too rich to be generated by proton activation, suggesting that fission on ^{226}Ra may occur in our activation condition. In addition, ^{140}Ba (β, $T_{1/2}$ = 12.6 d), a parent nuclide for ^{140}La, could also be generated as another fission product. Unfortunately, direct confirmation for the presence of ^{140}Ba was impossible in our sample, because most of characteristic gamma lines for ^{140}Ba were close to those of ^{214}Bi (RaC) and the chemical similarity between Ba and Ra, that always interfered to evaluate small amount of ^{140}Ba in large amounts of ^{226}Ra with its descendants. However, the primal separation of the ^{225}Ac fraction would practically eliminate ^{140}Ba along with ^{226}Ra due to chemical similarity. Indeed, orphan ^{140}La found in the ^{225}Ac fraction showed an acceptable half-life of 1.67 ± 0.10 d, and then decayed to a non-detectable level on the gamma spectrum by cooling for 2–3 weeks. This finding

suggests that the carrier Ba in Ra needles is not critical for the quality of ^{225}Ac, and no need for Ra purification from carrier Ba would be a practical advantage.

For example, we cooled the samples for 19–20 days after EOB or 2 weeks from the end of separation. The spectra of the cooled samples were similar to that for an authentic ^{225}Ac originating from a ^{229}Th/^{225}Ac generator [Figs. 4(b) and 4(c)]. The alpha spectrum of our ^{225}Ac product also showed the same profile as the reference (Fig. 5). Notably, neither ^{226}Ra ($E\alpha$ = 4.78 MeV, 94%) nor ^{210}Po ($E\alpha$ = 5.30 MeV, 100%) was detected. Hence, the double separation with an appropriate cooling period gave pure ^{225}Ac with a quality comparable to generator-made ^{225}Ac.

Recovery of ^{226}Ra for recycling

We developed a closed circuit for Ra recycling to minimize the loss of the ^{226}Ra inventory (Figs. 2 and 6). This process effectively reduced long-lived radioactive wastes. After single-runs of this circuit, we evaluated the ^{226}Ra leftover in each measurable material (i.e., the Ra recovery fraction), separation materials (cartridges), and reservoirs. The Ra recovery fraction contained 90–98% of ^{226}Ra, and other materials were negligible (e.g., < 1–2 μg (μCi) when handled with a 1000-μg ^{226}Ra batch). It should be noted that the Ra leftover depended on the volume of the residual liquid presented in the dead-space or on the surface. In addition, any deposition/leftover on the target box could not be estimated due to its high radioactivity. Consequently, about a 10% discrepancy in the activity distribution can be explained by this reason. Since the target box was used repeatedly, the practical loss of ^{226}Ra would be negligible.

Discussion

Radionuclidic purity – impact of ^{226}Ac in ^{225}Ac

^{226}Ac disintegrates by the pathways of β decay (83%), EC (17%), and trace α decay (6×10^{-3}), which breed ^{226}Th (α, $T_{1/2}$ = 30.6 min), ^{226}Ra, and ^{222}Fr (β, $T_{1/2}$ = 14.2 min), respectively. Among these, the longest half-life of ^{226}Ra would be the biggest concern when considering the preparation of ^{225}Ac-labeled injections. According to an ICRP Publication [16], the human body contains an estimated 31 pg (1.13 Bq) of ^{226}Ra, where 27 pg (0.99 Bq) is accumulated in the skeletal system (87%) and 2.3 pg (0.084 Bq)/day comes from dietary intake. Although any discussion on the radiation safety related to both ^{226}Ac and ^{226}Ra is beyond the scope of this study, we estimate the possible amount for ^{226}Ra generation as a decay product of ^{226}Ac that would be informative to discuss further clinical applications of ^{225}Ac as well as to consider the appropriate cooling time to address the acceptable quality on the ^{225}Ac product.

For simplicity, assuming a case where ^{226}Ac is the sole impurity in a 10-MBq ^{225}Ac product, a radionuclidic purity (RNP) of 68% (3.2-MBq (86-μCi) ^{226}Ac in ^{225}Ac) would finitely generate the same activity of ^{226}Ra in the whole body or a RNP 97.6% product (0.24-MBq (6.4-μCi) ^{226}Ac in ^{225}Ac) would be equal to that from a dietary path. At the end of the primal separation (4 d from EOB), the activity ratio of

$^{226}Ac/^{225}Ac$ in our samples ranged 1.4–2.3%, which is comparable to that in our dietary intake. As shown in Fig. 4(b), the secondary separation effectively increases the ^{225}Ac RNP, which reached > 99% within 2–3 weeks.

In addition, it would be worthwhile to mention that ^{227}Ac (β 98.6%, α 1.38%; T1/2 = 21.8 y), a major by-product in a spallation pathway from ^{232}Th target, would be a good reference to consider long-life alpha-emitting by-products. In the radioactivity-based estimation at the time of injection, ^{227}Ac is equivalent to 0.7% of ^{225}Ac [17] that would generate ^{223}Ra ($T_{1/2}$ = 11.4 d) through the alpha decay of ^{227}Th ($T_{1/2}$ = 18.7 d). A calculation on T_{max} (time for reaching the maximum activity) for ^{227}Th and ^{223}Ra are 164 d and 189 d, respectively, and the activity of ^{223}Ra would reach > 98% of the initial activity of ^{227}Ac at T_{max}. On the other hand, since ^{226}Ac has a shorter half-life than that of ^{227}Ac, the estimated T_{max} for ^{226}Ra is 23 d and at the T_{max} activity for ^{226}Ra would be 3.6×10^{-5}% of the initial activity of ^{226}Ac. However, these Ra activities generated from respective parents would be overestimated because above estimation did not take any biological excretion or metabolic paths into account. ^{226}Ra possibly generated from ^{226}Ac inside the body is seemed to be much smaller than ^{223}Ra from ^{227}Ac, and the activity of ^{226}Ra is a competitive magnitude to the naturally presented ^{226}Ra in our body; suggesting that any radiation risks caused by ^{226}Ac would be negligible or exceedingly small, if the RNP of ^{225}Ac is within or close to the range of our results.

Because the physical decay loss of ^{225}Ac during the cooling period is a critical issue for the ^{225}Ac industry, we plan to evaluate the biological impact of ^{226}Ac as a future feasibility study related to our ^{225}Ac product.

Conclusion

We obtained ^{225}Ac from an electrodeposited ^{226}Ra target. The ^{225}Ac purified with two separation columns showed an acceptable quality. The repeated separation process with appropriate cooling produced highly pure ^{225}Ac and byproducts were not detected.

The characteristics of the purified ^{225}Ac are similar to those of commercially available ^{225}Ac originating from a generator system. Thus, the proposed production method has potential as an alternative pathway to address the increasing demand for ^{225}Ac. The production results showed a linear increase of ^{225}Ac yield by increasing ^{226}Ra prepared, thus a clinical requirement of ^{225}Ac yield can be achieved by increasing the amount of ^{226}Ra, beam intensity, and irradiation period.

Declarations

ACKNOWLEDGEMENTS

The authors are grateful to our cyclotron staff for providing excellent beams. We also express our gratitude to Mikio Matsumoto, Hidetake Ishizu, Shogo Akabori, Kasumi Arai, and Takuya Shiina for their technical support. We thank Steffen Happel (TrisKem International) and Atsushi B Tsuji for the fruitful discussion.

FUNDING

This work was supported by JSPS KAKENHI [Grant Numbers JP26461814 (K.N.), JP17K10384 (K.N.), and JP20K08096 (K.N.)] and by AMED [Grant Number JP17pc0101014 (T.H.)].

CONFLICTS OF INTERESTS

The authors have no potential conflicts of interest to report.

ETHICS APPROVAL

This is a radioisotope production study without any biological materials, and no ethical approval is required.

CONSENT TO PARTICIPATE

There is no participant in this study, and consent is not required.

References

1. Parker C, Nilsson S, Heinrich D, et al., for the ALSYMPCA Investigators*. Alpha Emitter Radium-223 and Survival in Metastatic Prostate Cancer. *N Engl J Med.* 2013;369:213–223
2. Kratochwil C, Bruchertseifer F, Giesel FL, et al. ^{225}Ac-PSMA-617 for PSMA-Targeted α-Radiation Therapy of Metastatic Castration-Resistant Prostate Cancer. *J Nucl Med* 2016;57:1941–1944
3. Kassis AI and Adelstein SJ. Radiobiologic Principles in Radionuclide Therapy. *J Nucl Med* 2005;46:4S–12S
4. Poty S, Francesconi LC, McDevitt MR, Morris MJ, Lewis JS. α-Emitters for Radiotherapy: From Basic Radiochemistry to Clinical Studies—Part 1. *J Nucl Med* 2018;59:878–884
5. Boll RA, Malkemus D, Mirzadeh S. Production of actinium-225 for alpha particle mediated radioimmunotherapy. *Appl Radiat Isot* 2005;62:667–679
6. Apostolidis C, Molinet R, Rasmussen G, Morgenstern A. Production of Ac-225 from Th-229 for Targeted α Therapy. *Anal Chem* 2005;77:6288–6291
7. IAEA Technical meeting on ‘Alpha emitting radionuclides and radiopharmaceuticals for therapy’ June 24–28 (2013) [report] website http://www-naweb.iaea.org/napc/iachem/working_materials/TM-44815-report-Alpha-Therapy.pdf Accessed Sep 23, 2020

8. Griswold JR, Medvedev DG, Engle JW, et al. Large scale accelerator production of ^{225}Ac: Effective cross sections for 78–192 MeV protons incident on ^{232}Th targets. *Appl Radiat Isot* 2016;118:366–374
9. Apostolidis C, Molinet R, McGinley J, Abbas K, Möllenbeck J, Morgenstern A. Cyclotron production of Ac-225 for targeted alpha therapy. *Appl Radiat Isot* 2005;62:383–387
10. Melville G, Liu SF, Allen BJ. A theoretical model for the production of Ac-225 for cancer therapy by photon-induced transmutation of Ra-226. *Appl Radiat Isot* 2006;64:979–988
11. Melville G, Meriarty H, Metcalfe P, Knittel T, Allen BJ. Production of Ac-225 for cancer therapy by photon-induced transmutation of Ra-226. *Appl Radiat Isot* 2007;65:1014–1022
12. Melville G, Allen BJ. Cyclotron and linac production of Ac-225. *Appl Radiat Isot* 2009;67:549–555
13. Wayne Rasband, ImageJ 1.53a. Available https://imagej.nih.gov/ij/ Accessed Sep 17, 2020
14. National Nuclear Data Center, NuDat 2.8 website https://www.nndc.bnl.gov/nudat2/chartNuc.jsp Accessed Sep 24, 2020
15. TALYS-based evaluated nuclear data library (TENDL-2019) website https://tendl.web.psi.ch/tendl_2019/proton_html/Ra/ProtonRa226xs.html Accessed Sep 4, 2020
16. International Commission on Radiological Protection, Limits for intakes of radionuclides by workers: ICRP Publication 30 (Part 1) website https://journals.sagepub.com/doi/pdf/10.1177/ANIB_3_3-4 Accessed Sep 5, 2020
17. Sgouros G, Frey E, He B, Ray N, Ludwig D. Dosimetric Impact of Ac-227 in Accelerator-Produced Ac-225 [abstract] J Med Imaging Radiat Sci 2019;50(suppl):S37–S38

Tables

TABLE 1 Production results

Run	#1	#2	#3
Beam condition (Ep=15.6 MeV)	20 μA x 3 h	20 μA x 5 h	20 μA x 5 h
Ra-deposition			
^{226}Ra, initial electrolyte	14.5 MBq (391 μCi)	36.4 MBq (984 μCi)	38.8 MBq (1.05 mCi)
^{226}Ra, deposited	13.5 MBq (366 μCi)	35.4 MBq (956 μCi)	37.5 MBq (1.01 mCi)
Deposition rate (%)	94	97	97
Nuclides of interest* in the primally purified sample (kBq, decay corrected to EOB)			
^{225}Ac (150 keV, 0.6%)	522	2.23 x10^3	2.43 x10^3
^{226}Ac (230 keV, 26.9%)	111	451	488
^{226}Ra (186 keV, 3.64%)	not detected	not detected	not detected
^{214}Pb (352 keV, 35.6%)	not detected	not detected	not detected
^{214}Bi (609 keV, 45.5%)	5.2	13.5	33.3
^{135}La (481 keV, 1.52%)	84.5	333	344
^{140}La (487 keV, 43.9%)	0.0571	0.165	0.231

* Nuclear data presented in parenthesis [14], were used for quantification.

Quantification was performed on a 4096-ch well calibrated HPGe, where the uncertainty and detection limit were 9% and 3.7 Bq (1.2×10^{-3}% of ^{225}Ac in the most sensitive case), respectively.

Figures

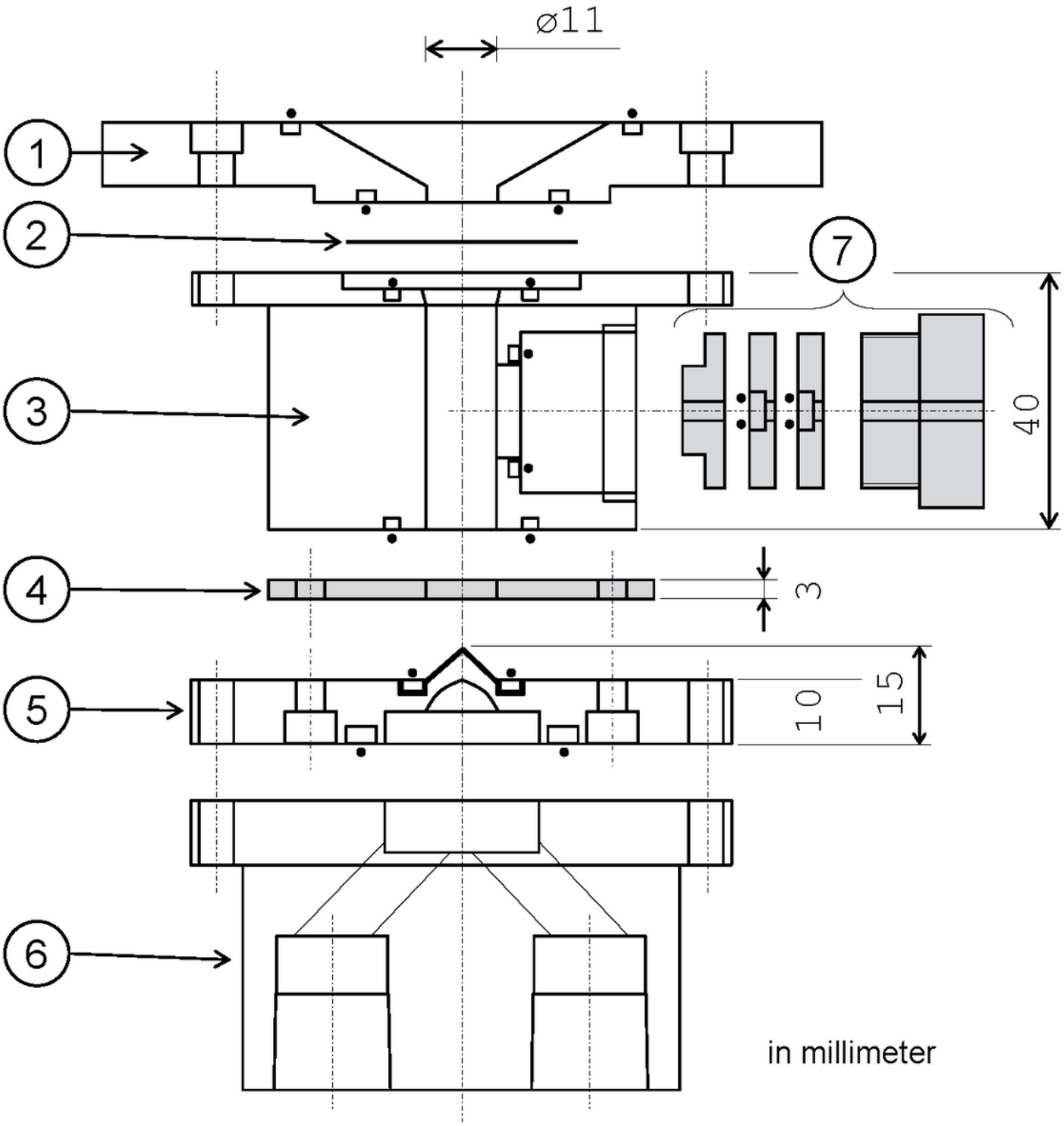

Figure 1

226Ra target assembly

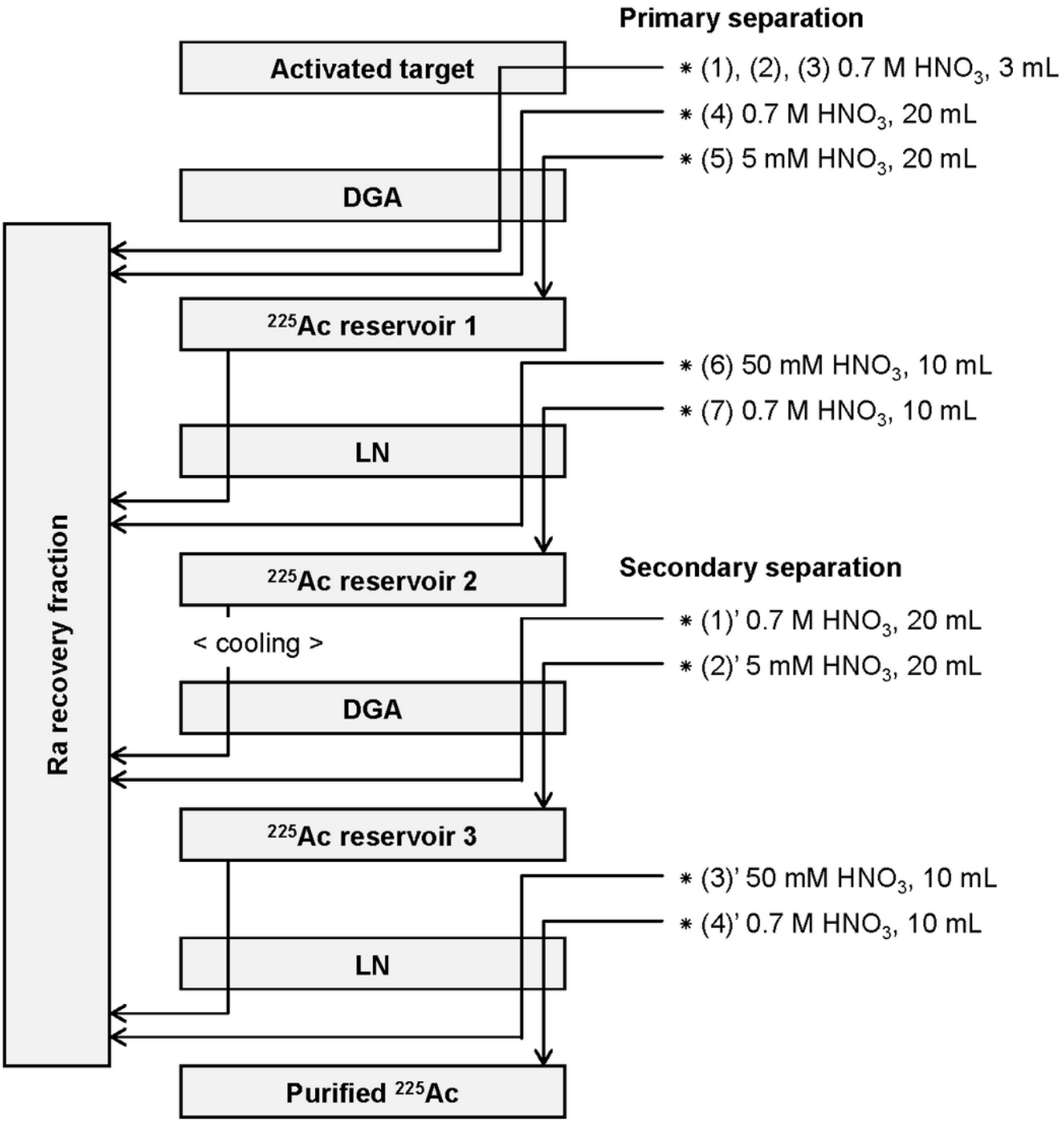

Figure 2

Separation diagram for 225Ac from a 226Ra matrix

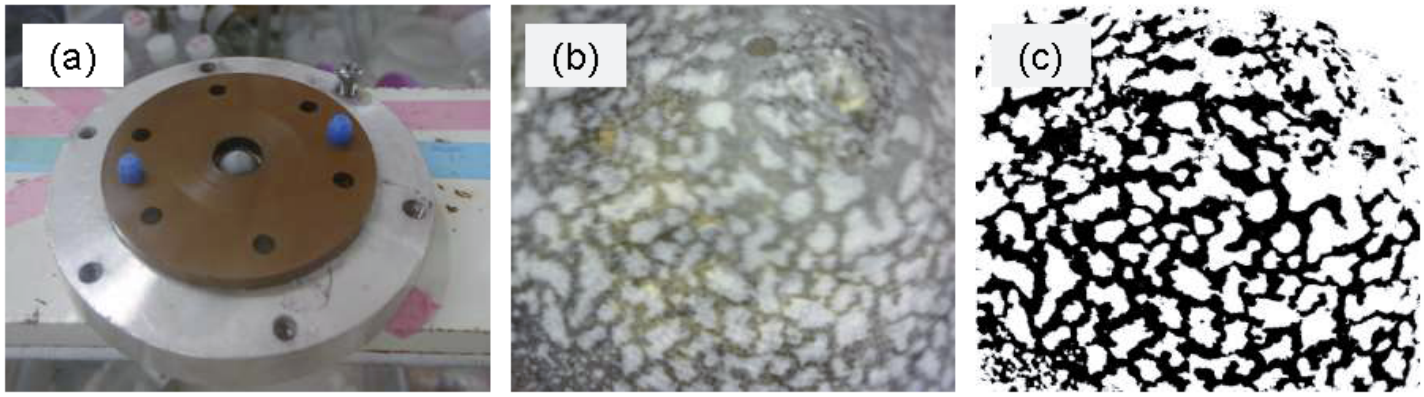

Figure 3

Deposition result of approximately 1000 µg (µCi) of 226Ra on the target surface (cathode) after drying. (a) Photograph of the target surface with an electric insulator (b) Magnification (30×) of the deposition surface (c) Enhanced monochrome image (64% of the surface is estimated to be covered by sediment)

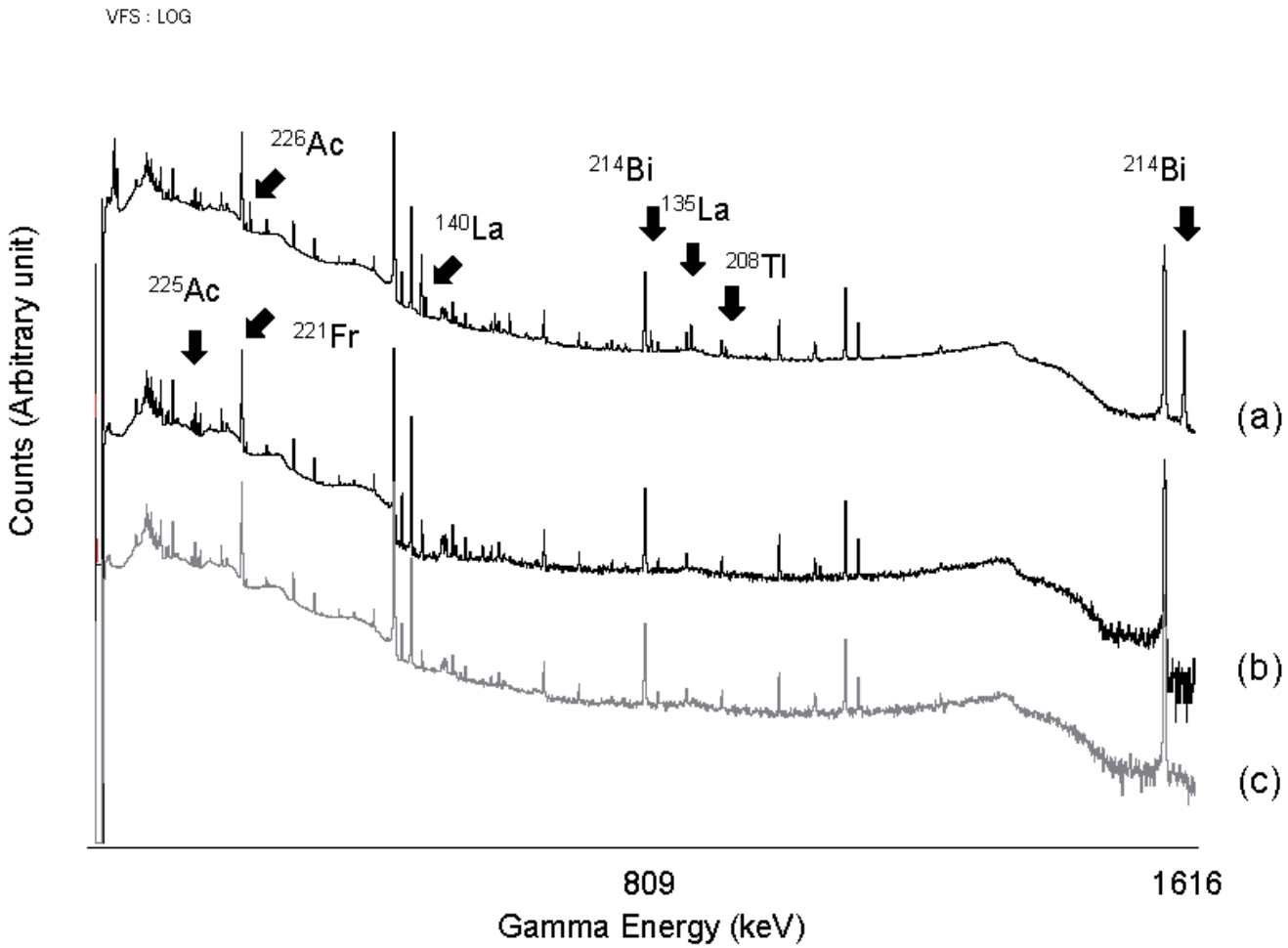

Figure 4

Gamma spectrum for various 225Ac samples (a) 225Ac product (primary separation) after 4 d from EOB (b) 225Ac product (secondary separation) after 20 d from EOB (c) Commercially available authentic 225Ac (generator-made)

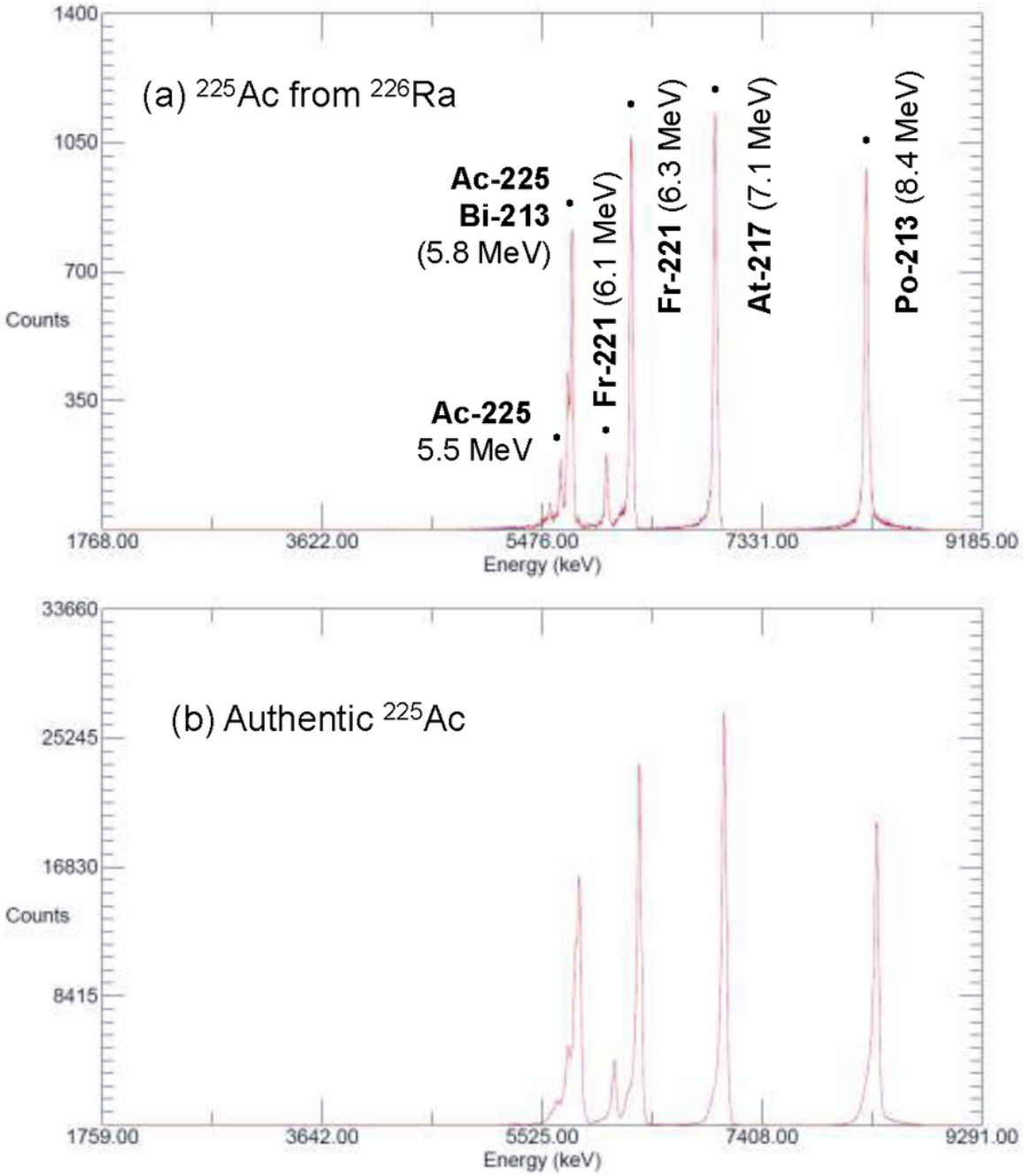

Figure 5

Alpha spectrum for the 225Ac product Aliquot of 0.37–1.85-kBq 225Ac dried on an Al disk measured without a covering. (a) Purified 225Ac product after 19 d from EOB (b) Commercially available authentic

225Ac

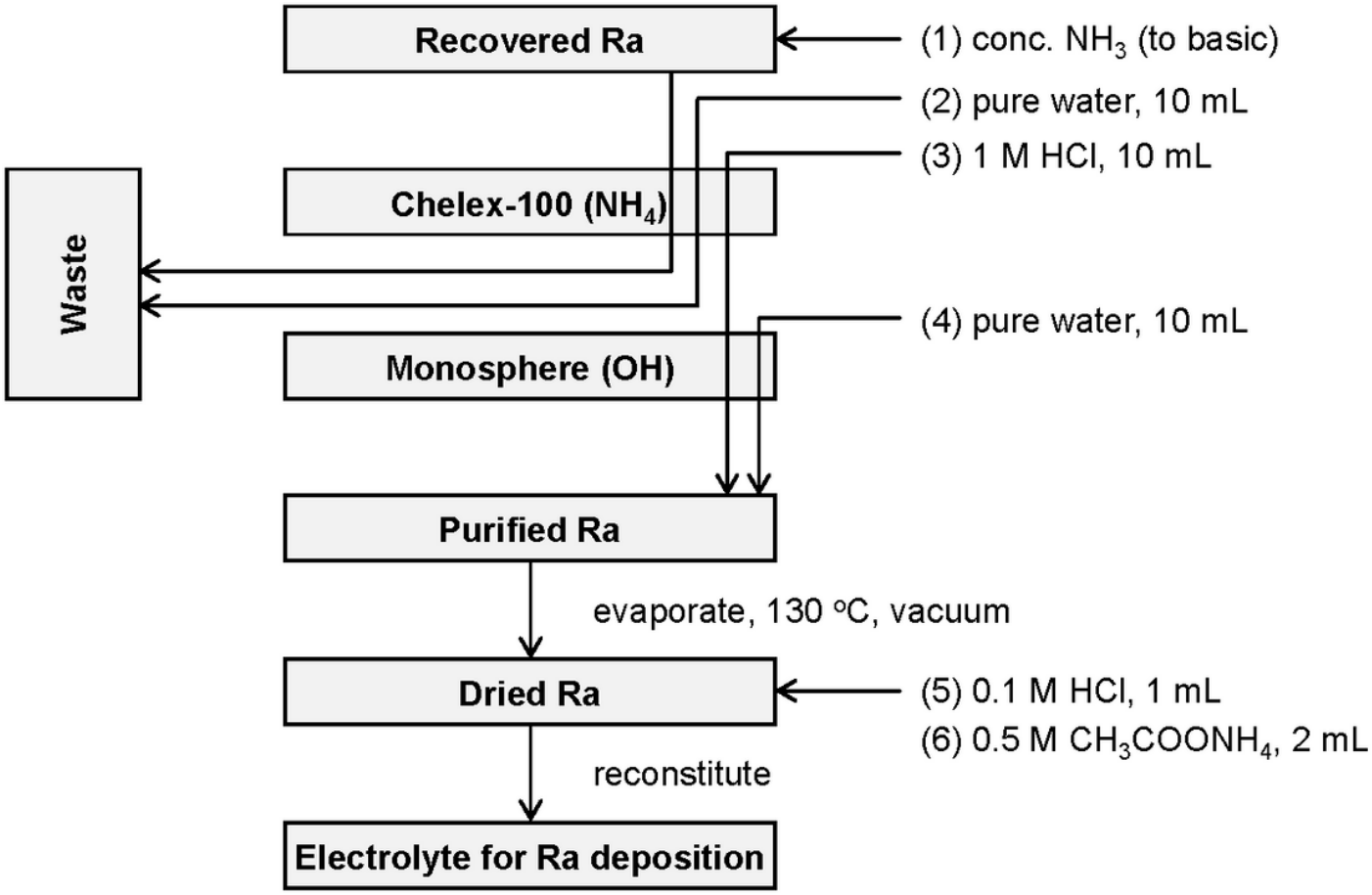

Figure 6

Diagram of 226Ra recycling

Supplementary Files

This is a list of supplementary files associated with this preprint. Click to download.

- Nagatsuonlineresource.pdf